

## Preliminary Results from a Trace-Element Study of Amphibole-Cumulate Rocks from the Bonanza Arc, Vancouver Island, British Columbia (NTS 092A/09)

R.J. D'Souza, School of Earth and Ocean Science, University of Victoria, Victoria, BC, rdsouza@uvic.ca

D. Canil, School of Earth and Ocean Science, University of Victoria, Victoria, BC

---

D'Souza, R.J. and Canil, D. (2015): Preliminary results from a trace-element study of amphibole-cumulate rocks from the Bonanza Arc, Vancouver Island, British Columbia (NTS 092A/09); *in* Geoscience BC Summary of Activities 2014, Geoscience BC, Report 2015-1, p. 103–110.

### Introduction

Porphyry-Cu deposits, which are closely associated with convergent-margin (i.e., arc) settings, are sources for much of the world's Cu and almost the entire supply of the world's Mo (Sinclair, 2007). Rare metals, including Pt, Pd and W, are also found in porphyry-Cu systems. However, despite the genetic association of such deposits with convergent margins, not all arcs are prospective for the formation of porphyry-Cu deposits. For example, the Jurassic Bonanza Arc on northern Vancouver Island hosted the Island Copper mine (Canada's third largest, active from 1970 to 1995), but no similar deposit has been discovered elsewhere on Vancouver Island, despite the extensive exposure of the Bonanza Arc rocks.

The key to whether or not magmas are enriched in Cu depends critically on the oxidation state of the magma and the speciation of S. Under reducing conditions, S is present as sulphide and the chalcophile elements (Cu, Au, Mo, etc.) are sequestered in the immiscible sulphide melt and lost from the magma. Under more oxidizing conditions, however, S is present as sulphate and thus Cu remains in the silicate magma. A recent study by Chiaradia (2014) reported that arcs with crust >30 km in thickness tend to produce Cu-poor volcanic rocks, whereas arcs <20 km in thickness produce Cu-rich volcanic rocks, contrary to prior observations of porphyry deposits with thick arcs (e.g., Sinclair, 2007; Sillitoe, 2010). Chiaradia (2014) attributed his observations to magnetite fractionation at depth from water-rich magmas, which would produce a reduced magma in which sulphide is stable and able to remove the chalcophile elements. This produces a sulphide-rich lower crust that could be melted by later magmas to produce porphyry-Cu deposits (Lee et al., 2012; Chiaradia, 2014).

In addition to their association with economic ore deposits, arcs are also thought to be the locus of continental growth, based on the similarity between the andesitic bulk composition of arcs and that of the bulk continental crust (e.g., Taylor, 1977; Rudnick and Fountain, 1995; Rudnick and Gao, 2014). However, Lee et al. (2012) noted some discrepancies between these compositions. Specifically, the bulk continental crust is depleted in Cu, Sc, Ni and Cr relative to parental arc magmas. Whereas Cu depletion is likely due to sulphide fractionation, Lee et al. (2012) postulated that the coupled depletion in Sc, Cr and Ni indicates the effect of pyroxene or amphibole fractionation in the lower crust of arcs. Amphibole fractionation in the lower crust of arcs would effectively filter ascending magmas of up to 20% of their water and form a fertile, incompatible-element-rich lower crust (Davidson et al., 2007). Release of this water from this 'sponge' could enhance melt production in the lower crust (Davidson et al., 2007) and promote the melting of sulphides to produce the Cu-rich melts that could form porphyry-Cu deposits (Chiaradia, 2014).

This paper describes the results of preliminary work to test the hypotheses of Davidson et al. (2007) and Lee et al. (2012) using intrusive rocks of the Jurassic Bonanza Arc exposed on Vancouver Island. Trace-element chemistry of amphiboles and pyroxenes from sulphide-bearing, amphibole-rich cumulate ultramafic rocks that have been described in the Bonanza Arc by Larocque and Canil (2010) is examined to determine whether amphibole crystallization could control magma evolution. The origin of amphibole in these rocks is contentious, with arguments having been made for both primary (e.g., Larocque and Canil, 2010) and secondary (e.g., Fecova, 2009) origin.

A recent study by Smith (2014) on lower crustal xenoliths in volcanic rocks from the Solomon Islands concluded that the amphibole in those samples was formed by melt reaction of primary clinopyroxene. Trace-element distributions in the cumulate rocks from the Bonanza Arc may indicate whether amphibole is a primary fractionating phase or a secondary melt-reaction product. Answers to this question provide an important test of the hypothesis that amphibole crystallization can drive the chemical evolution of an arc

---

**Keywords:** geochemistry, Bonanza Arc, amphibole, pyroxene, sulphides

This publication is also available, free of charge, as colour digital files in Adobe Acrobat® PDF format from the Geoscience BC website: <http://www.geosciencebc.com/s/DataReleases.asp>.

(Davidson et al., 2007). If the amphibole in the Bonanza Arc cumulate rocks is a primary magmatic phase, this would imply the existence of water-rich, incompatible-element-rich, lower crustal rocks that could have been the source of later magmas that formed porphyry-Cu deposits (Chiaradia, 2014).

### Industry Application

In addition to testing whether amphibole is indeed controlling the magma evolution and behaviour of incompatible elements in the lower crust, as predicted by Davidson et al. (2007) and Lee et al. (2012), this study will contribute to the understanding of the processes by which some arcs and not others are prospective for the formation of porphyry-Cu deposits. The observation by Chiaradia (2014) of the inverse relationship between volcanic Cu content and arc thickness is not consistent with the observation of porphyry-Cu deposits in association with thick arcs. Testing the hypothesis postulated by Chiaradia (2014) for this inverse relationship has the potential to refine current exploration strategies and expand understanding of the formation of these deposits.

### Regional Geology

The Jurassic Bonanza Arc on Vancouver Island (Figure 1) was emplaced within a pre-Jurassic crust comprising a Triassic oceanic plateau (the Karmutsen basalts) and a Devonian arc (the Sicker Group; Muller and Yorath, 1977). A compilation of U-Pb (zircon) and Ar-Ar (hornblende) ages from the Bonanza Arc (D'Souza et al., work in progress) shows that the arc was emplaced between 203 and 160 Ma, with a large peak at 170 Ma. Although the Bonanza Arc is considered to be correlative with the Jurassic Talkeetna Arc in Alaska (DeBari et al., 1999), the Talkeetna Arc differs in that it was emplaced directly on oceanic crust (DeBari and Coleman, 1989). Rare garnet-bearing cumulate rocks have

also been discovered within the Talkeetna Arc section but have not been reported from the Bonanza Arc (DeBari et al., 1999).

The Bonanza Arc consists of volcanic rocks and their plutonic counterpart, which has traditionally been divided into two groups: the Westcoast Crystalline Complex and the Island Plutonic Suite (Muller and Yorath, 1977). The volcanic rocks consist of basalt, andesite, dacite and rhyolite that have been emplaced as flows, breccias and tuffs. The Westcoast Crystalline Complex is a variably foliated unit comprising hornblendite, gabbro and granodiorite. Application of Al-in-hornblende barometry indicates that this unit equilibrated at depths of 10–17 km (with high uncertainty; Canil et al., 2010). The Island Plutonic Suite is typically unfoliated and, on average, more felsic than the Westcoast Crystalline Complex; the former comprises quartz diorite, granodiorite, quartz monzonite and tonalite. The Island Plutonic Suite was emplaced at depths of 2–10 km, as indicated by Al-in-hornblende barometry (Canil et al., 2010). Aside from the presence of foliation, the distinction between the Island Plutonic Suite and the Westcoast Crystalline Complex is, in practice, difficult to observe in the field. Amphibole-rich cumulate rocks have been reported as schlieren and layers within intermediate plutonic rocks.

### Amphibole in the Bonanza Arc: Primary or Melt-Reaction Product?

On the basis of geochemical modelling, Fecova (2009) concluded that the amphibole in the Bonanza Arc was a product of reaction between primary clinopyroxene and a later melt. Similarly, DeBari and Coleman (1989) and Greene et al. (2006) interpreted the amphibole in plutonic rocks from the Talkeetna Arc as not being primary but instead to have formed as a result of fluid enrichment, melt reaction or subsolidus re-equilibration of cumulus clinopyroxene. Conversely, Larocque and Canil (2010) argued that the major-element geochemistry indicates that amphibole is a primary fractionating phase in the Bonanza Arc. D'Souza et al. (work in progress) determined a Rb-Sr isochron age for samples of the Bonanza Arc (including amphibole-bearing ones) of ca. 160 Ma, coinciding with the age of magmatism. They argued that the closeness of the Rb-Sr isochron age and the emplacement age supports the argument that amphibole is a primary fractionating phase in these magmas, as the Rb-Sr isochron would have been reset by amphibole formation by reaction of clinopyroxene with a later melt. Petrographic evidence appears equivocal (Fecova, 2009; Larocque and Canil, 2010) because clinopyroxene is observed to grade into amphibole in some samples, indicating a fluid-reaction origin, whereas chadacrysts of amphibole are seen within oikocrysts of relatively pristine olivine in other samples, implying a primary origin (Figure 2).

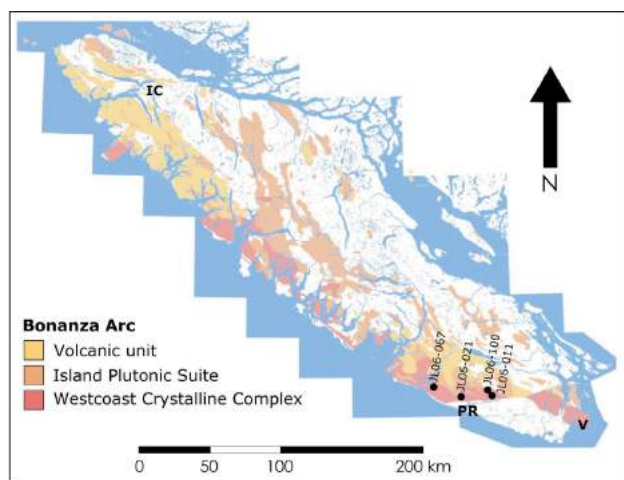


**Figure 1.** Simplified geology of Vancouver Island, showing the Jurassic Bonanza Arc and pre-existing igneous rocks. Locations of samples analyzed in this study are shown and labelled. Abbreviations: IC, Island Copper minesite; PR, Port Renfrew; V, Victoria.

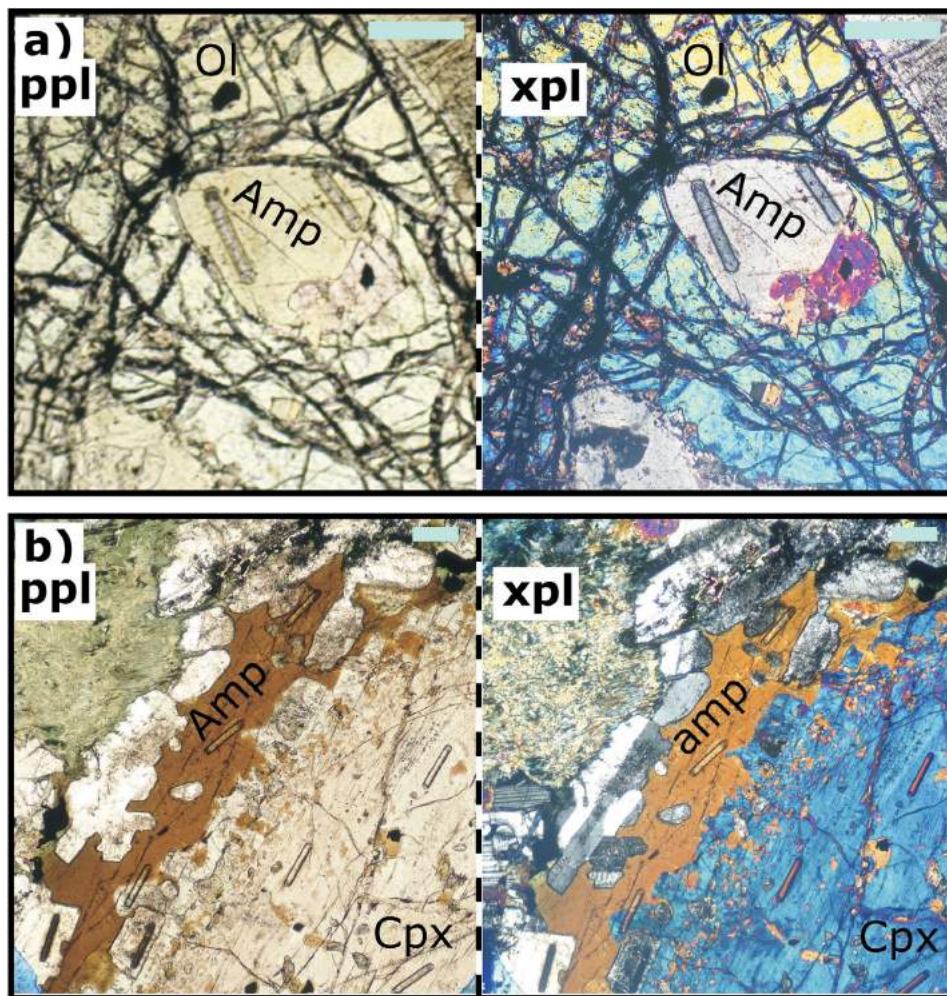


**Figure 2.** Photomicrographs of **a)** an amphibole chadacryst within an olivine oikocryst, JL06-021; **b)** a gradational contact between amphibole and clinopyroxene, JL06-100. Scale bar in all images is 200  $\mu\text{m}$ , the length of the ablation pits in the images. Images shown were taken in plane polarized light (ppl) and cross-polarized light (xpl).

## Methods

Trace-element compositions were analyzed for amphibole, clinopyroxene, orthopyroxene and plagioclase in four amphibole-bearing cumulate samples (Table 1) from exposures near Port Renfrew for which mineral chemistry and bulk-rock compositions are available (Larocque, 2008; locations in Figure 1). These samples were selected because they contained all the phases of interest and also appeared under the microscope to show little alteration.

Rare-earth-element (REE) and other trace-element concentrations were determined at the School of Earth and Ocean Sciences, University of Victoria using a New Wave Research UP213 laser-ablation system and a Thermo X-Series II inductively coupled plasma-mass spectrometer with an argon-gas carrier system. Four ablation passes were conducted along a raster line that was 200  $\mu\text{m}$  long and 40  $\mu\text{m}$  wide, using an average laser power of  $\sim 14 \text{ J/cm}^2$ . Gas-blank compositions were also determined for every analysis and

United States Geological Survey standard glass BCR2g was analyzed after every six to eight analyses. The BCR2g standard glass and National Institute of Standards and Technology (NIST) standard glasses 615, 613 and 611 were analyzed at the start and end of every sample. These standards were analyzed under the same conditions used for phases in the samples.

After data collection, the individual spectra of counts per second versus time were examined for each analysis and sections that showed flat plateaus were manually selected. Ramps and saw-tooth patterns in such spectrum were edited, as they are likely due to laser or plasma instability and the presence of unseen inclusions, respectively. The data were reduced to concentrations in parts per million in a spreadsheet using Ca and Si concentrations (determined by microprobe; Larocque, 2008) as internal standards. All analyses were also corrected for instrument drift using the analyses of BCR2g collected during the session. GeoReM (Jochum

**Table 1.** Petrographic summary of the samples analyzed in this study, from exposures near Port Renfrew.

Sample	Rock type	Mineralogy (mode - species)				
		Amphibole	Pyroxene	Feldspar	Olivine	Other
JL06-021	Olivine cumulate	62% - tschermakite	6% - enstatite, diopside	20% - plagioclase	12% - chrysotile	-
JL06-011	Plagioclase cumulate	60% - magnesiohornblende, tschermakite	23% - enstatite, diopside	12% - An <sub>53-90</sub> Ab <sub>10-53</sub> Or <sub>0-8</sub>	-	5% - Fe-Ti oxide
JL06-067	Plagioclase cumulate	64% - magnesiohornblende, tschermakite	3% - diopside	30% - An <sub>52-92</sub> Ab <sub>9-48</sub> Or <sub>0.5-1</sub>	-	1% - Fe-Ti oxide; 2% - biotite
JL06-100	Plagioclase cumulate	29% - tschermakite	6% - augite, diopside	65% - An <sub>46-54</sub> Ab <sub>46-51</sub> Or <sub>0.6-4</sub>	-	-

et al., 2005) preferred values were used for the NIST and BCR2g standard element concentrations.

## Results

Chondrite-normalized REE profiles (Figure 3) for the amphibole and pyroxene in all four samples are convex upward, with the apex at Sm. This convex-upward shape is similar to the shape of the REE profile for the JL06-011 and JL06-021 whole-rock analyses, reflecting the high proportion of amphibole and pyroxene in these samples. There are two amphibole populations in sample JL06-067: one that is similar in profile curvature to the amphibole in the other samples (dark green on Figure 3) and another that shows higher La and Ce abundances, and therefore has less curved profiles (light green on Figure 3).

The two populations of amphibole are also evident on a plot of the Eu anomaly (calculated using Equation 1, where Eu\* is the expected Eu abundance, given the observed chondrite-normalized Sm and Gd abundances) versus the chondrite-normalized La/Sm ratio (Figure 4). The amphibole analyses show varying Eu anomalies, from positive (JL06-021) to none or slightly negative (JL06-011, JL06-021) to strongly negative (JL06-100). A strong negative correlation was observed between the Eu anomaly and La/Sm ratio in the main amphibole population, except for the subvertical array described by amphiboles from JL06-021 (i.e., amphiboles that are both chadacrysts within olivine oikocrysts and oikocrysts to olivine chadacrysts). The high La/Sm population of amphibole from JL06-067 shows a small range in Eu anomaly (1.1–1.3) and little variation with La/Sm ratio.

$$Eu/Eu^* = Eu_N / ((Sm_N + Gd_N) / 2) \quad (1)$$

The pyroxenes have REE profiles that are similar in shape (i.e., convex upward, Figure 3) to the amphiboles. The pyroxenes have lower REE abundances than the amphiboles, except in JL06-011, where the middle and heavy REE (Sm to Lu) abundances of amphibole and pyroxene overlap. Pyroxene in JL06-011 and JL06-067 shows larger, negative Eu anomalies than amphibole, whereas the opposite is observed in JL06-100. In Figure 4, the pyroxene shows a range in La/Sm ratio similar to that of the amphibole (ex-

cept the high La/Sm amphibole from JL06-067). In Figure 4, the Eu anomalies in the pyroxene data fall within the range of those in the amphibole data but are more restricted (0.6–1.1) and do not display any strong trends.

On a plot of the extended trace-element profiles (normalized to primitive-mantle values; Figure 5), the most striking features are the sharp negative Cu and Zn anomalies that are seen in the analyzed phases of all samples. The values for MnO, MgO and FeO\* on Figure 5 are averaged from the microprobe data for each phase in a given sample. Within each sample, the trace-element profiles for amphibole and pyroxene are remarkably similar, with the only noticeable difference being that amphibole generally shows higher Co and V abundances than pyroxene.

Whereas two amphibole populations in JL06-067 are visible in Figures 3 and 4, these same populations are not easily distinguished in the extended trace-element profiles (Figure 5). The amphibole analyses that constitute the high-La/Sm population have been highlighted in light green on Figure 5 and show generally lower Yb, Lu, Y, V and Cu than the low-La/Sm amphibole population. There are, however, no consistent and distinct differences between these two amphibole populations in Figure 5.

## Discussion

The convex-upward shape of the REE profiles of the amphibole (Figure 3) is similar to those of the pyroxene, except that the latter are flatter in the middle to heavy REE (Sm to Lu). These profiles reflect the high partition coefficients for amphibole and pyroxene (relative to basaltic melt) for the middle and heavy REE, respectively (Green et al., 2000; Tiepolo et al., 2007). The relative enrichments and shape of the REE profiles of the amphibole and pyroxene in the present study are similar to those reported by Smith (2014) for amphibole and pyroxene from cumulate nodules in volcanic rocks on the Solomon Islands.

As both phases have generally similar partition coefficients for the REE (Green et al., 2000; Tiepolo et al., 2007), some differences between the profiles of these two phases, notably the Eu anomaly (Figure 4), are important. Except for amphibole from JL06-021 and the high La/Sm population

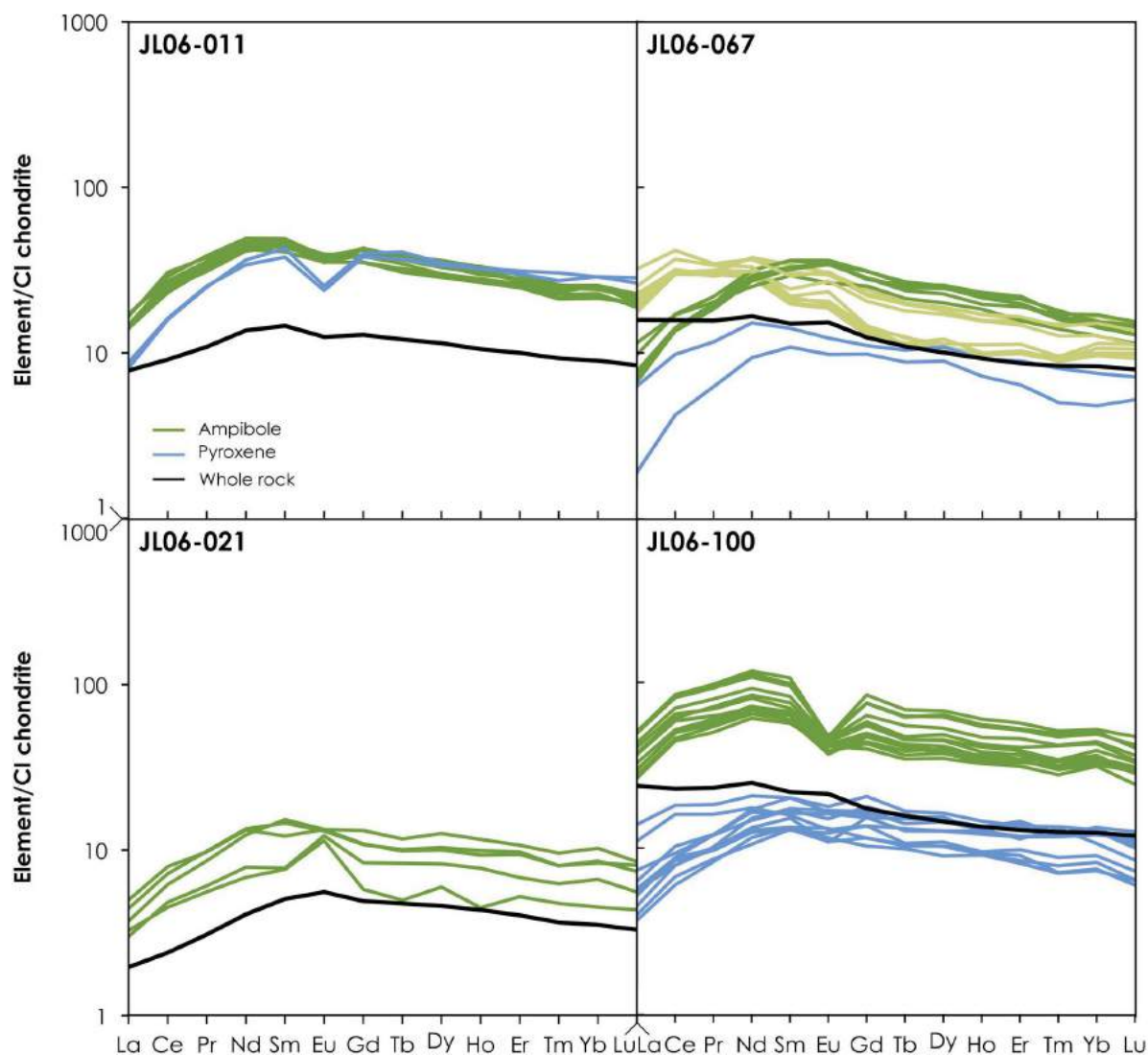


**Figure 3.** Chondrite-normalized (McDonough and Sun, 1995) rare-earth-element (REE) profiles for amphibole, pyroxene and the whole rock in each sample analyzed in this study. Amphiboles in JL06-067 are separated into two groups on the basis of REE-profile shape, as discussed in the text.

from JL06-067, the Eu anomaly in amphibole becomes more negative as the REE profile between La and Sm becomes flatter (i.e.,  $Eu/Eu^*$  decreases as  $La/Sm$  increases). A negative Eu anomaly is commonly attributed to the crystallization of plagioclase from a melt, as Eu is very compatible in that phase. In individual samples and in the entire dataset (except for JL06-021 and the high- $La/Sm$  population in JL06-067), the  $La/Sm$  ratio of the amphibole increases continuously (Figure 4) due to the simultaneous increase in La and Sm concentration, albeit at different rates (Figure 6). The increasingly negative Eu anomaly might be consistent with continuous amphibole production prior to and during plagioclase crystallization. The increasing La and Sm concentration of amphibole (Figure 6) is in accord with this idea, as these elements are incompatible in plagioclase. Furthermore, amphibole displays Eu anom-

alies that are less negative compared to pyroxene in JL06-011 (Figures 3, 6), implying that amphibole may have crystallized prior to or during plagioclase crystallization, which itself occurred prior to clinopyroxene crystallization.

The high- $La/Sm$  amphibole population from JL06-067 describes a subhorizontal trend on Figure 4. The same population also shows only a small range in Sm content but a much larger range in La (Figure 6), which is correlated positively with the Eu anomaly. The similarity of the REE abundance and profile shape of these amphiboles (Figure 3) to those from analyses of ‘amphibole rim on nodule’ (Daniel, 2014) likely points to a similar origin, presumably by reaction with melt. Such an origin might also be responsible for the higher Co concentration observed in the high- $La/Sm$  amphibole population in JL06-067 (Figure 5).

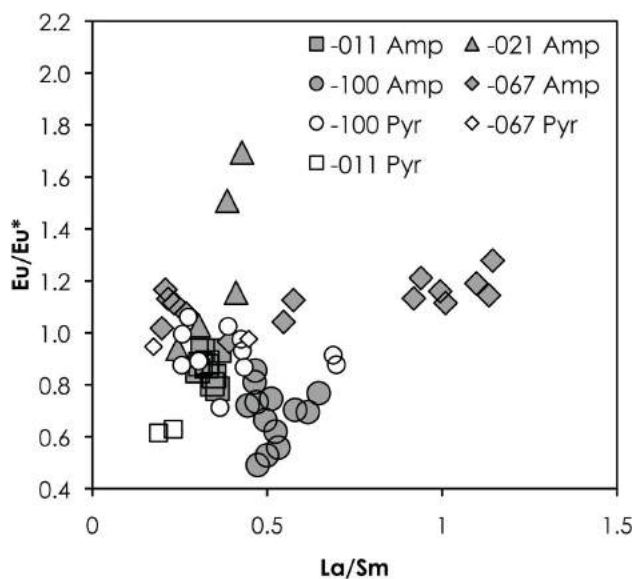


**Figure 4.** Eu anomaly versus La/Sm ratio of the amphibole and pyroxene in each sample analyzed in this study. Both ratios are chondrite normalized (McDonough and Sun, 1995). See text for calculation of the Eu anomaly.

Pyroxene analyses have Eu anomalies ranging from slightly positive to slightly negative and show no variation with increasing La/Sm (Figure 4). The increase in La/Sm for the pyroxenes is due mainly to an increase in their La concentration, as Sm content stays generally constant within a sample (Figure 6). The lack of variation in the pyroxene Eu anomaly (Figure 4) may imply that pyroxene crystallization occurred over a small window straddling the onset of plagioclase crystallization. Additionally, pyroxene analyses from samples JL06-067 and JL06-100 plot as a subvertical array that is continuous with analyses of amphibole from JL06-021 (Figure 6b), which could indicate that the amphibole in JL06-021 crystallized before plagioclase, whereas the pyroxene crystallized after. Another possibility is that the amphibole in JL06-021 was originally pyroxene that reacted with a later-transiting melt to form amphibole, although this explanation is at odds with the observation that some amphibole in this sample forms as chadacrysts within olivine oikocrysts.

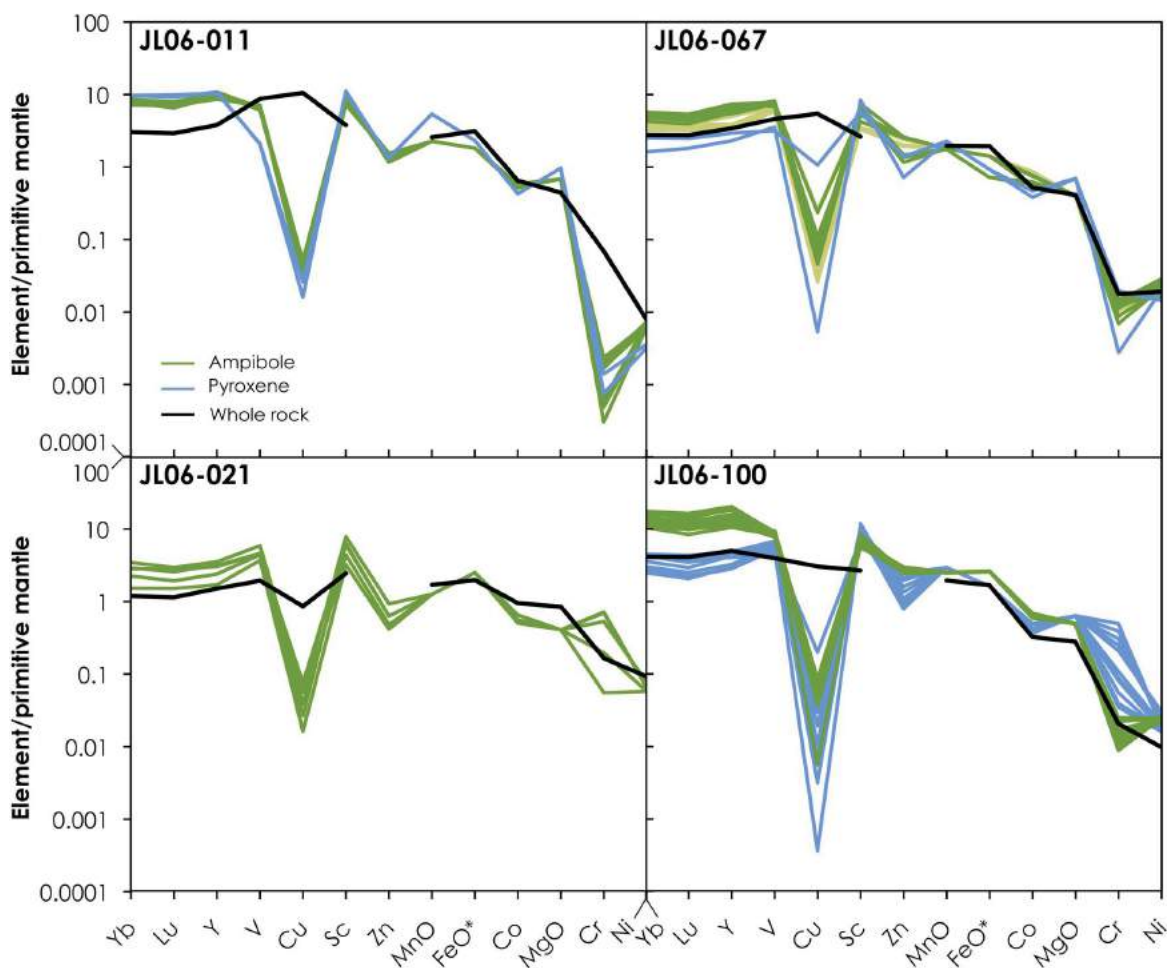


**Figure 5.** Primitive-mantle-normalized (Palme and O'Neill, 2014), extended trace-element profiles for amphibole, pyroxene and the whole rock in each sample analyzed in this study.

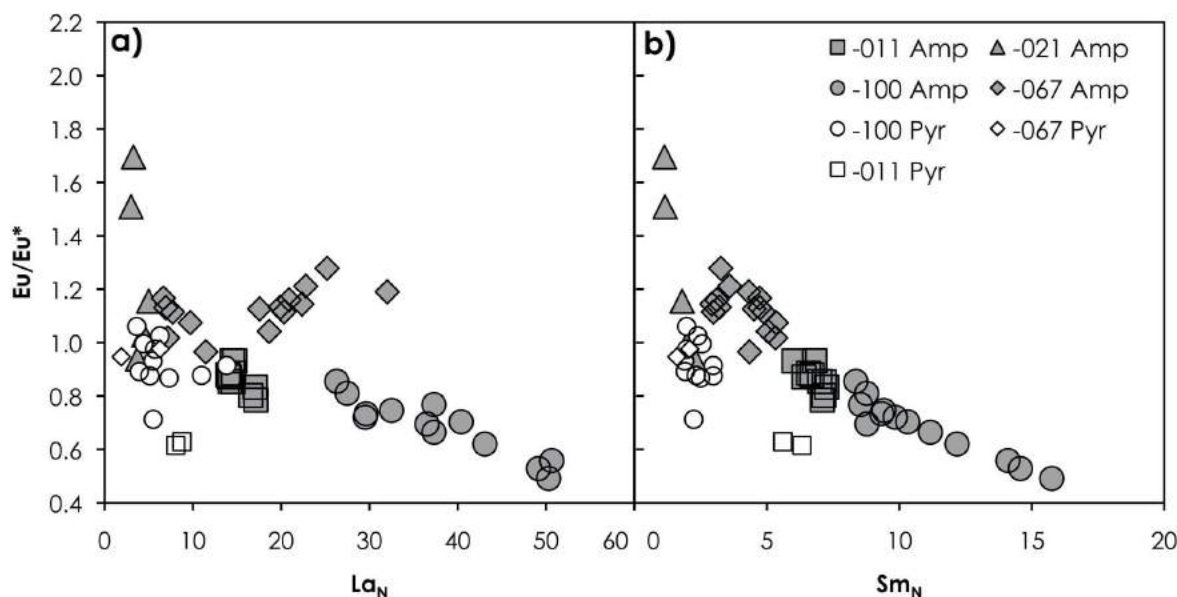


**Figure 6.** Europium anomaly versus La (a) and Sm (b) concentration of the amphibole and pyroxene analyzed in this study.

## Conclusions

The authors' interpretations indicate that amphibole in some plagioclase cumulates crystallized prior to plagioclase and pyroxene (i.e., the low-La/Sm amphiboles from sample JL06-067), during plagioclase crystallization but before pyroxene (JL06-011), or after plagioclase and pyroxene crystallization (JL06-100). Some amphiboles (e.g., high-La/Sm amphibole from JL06-067) show REE and trace-element concentrations that could imply that the amphibole was produced by reaction of pyroxene with a later melt. The origin of amphibole in JL06-021 is enigmatic, as it is present as chadacrysts within olivine and as oikocrysts to olivine; however, both populations show pyroxene-like variation in Eu anomaly, La/Sm ratio and abundance of La and Sm.

## Future Work

Analyses of the trace-element abundances in amphibole from other samples, as well as analyses of the coexisting olivine, plagioclase, sulphides and magnetite, are planned in the near future. This work will help in elucidating the role of H<sub>2</sub>O and amphibole crystallization along the liquid lines of descent in the Bonanza Arc magmas and their role in causing magnetite or sulphide saturation in the arc crust. The latter phases may have played a role in chalcophile abundance in Bonanza Arc magmas (Chiaradia, 2014).

## Acknowledgments

The authors thank J. Spence for assistance and training in data collection and reduction using the laser-ablation inductively coupled plasma-mass spectrometer at the University of Victoria. Thanks also go to A. Locock and A. Blinova for thoughtful reviews of this study.

## References

- Canil, D., Styan, J., Larocque, J., Bonnet, E. and Kyba, J. (2010): Thickness and composition of the Bonanza arc crustal section, Vancouver Island, Canada; *Geological Society of America Bulletin*, v. 122, p. 1094–1105.
- Chiaradia, M. (2014): Copper enrichment in arc magmas controlled by overriding plate thickness; *Nature Geoscience*, v. 7, p. 43–46, doi:10.1038/ngeo2028
- Davidson, J., Turner, S., Handley, H., MacPherson, C. and Dosseto, A. (2007): Amphibole “sponge” in arc crust?; *Geology*, v. 35, p. 787–790.
- DeBari, S.M. and Coleman, R.G. (1989): Examination of the deep levels of an island arc: evidence from the Tonsina ultramafic assemblage, Tonsina, Alaska; *Journal of Geophysical Research*, v. 94, p. 4373–4391.
- DeBari, S.M., Anderson, R.G. and Mortensen, J.K. (1999): Correlation among lower to upper crustal components in an island arc: the Jurassic Bonanza arc, Vancouver Island, Canada; *Canadian Journal of Earth Sciences*, v. 36, p. 1371–1413.
- Fecova, K. (2009): Conuma River and Leigh Creek intrusive complexes: windows into mid-crustal levels of the Jurassic Bonanza arc, Vancouver Island, British Columbia; M.Sc. thesis, Simon Fraser University, 245 p.
- Green, T.H., Blundy, J.D., Adam, J. and Yaxley, G.M. (2000): SIMS determination of trace element partition coefficients between garnet, clinopyroxene and hydrous basaltic liquids at 2–7.5 GPa and 1080–1200°C; *Lithos*, v. 53, p. 165–187.
- Greene, A.R., DeBari, S.M., Kelemen, P.B., Blusztajn, J. and Clift, P.D. (2006): A detailed geochemical study of island arc crust: the Talkeetna arc section, south-central Alaska; *Journal of Petrology*, v. 47, p. 1051–1093.
- Jochum, K.P., Nohl, U., Herwig, K., Lammel, E., Stoll, B. and Hofmann, A.W. (2005): GeoReM: a new geochemical database for reference materials and isotopic standards; *Geostandards and Geoanalytical Research*, v. 29, p. 333–338.

- Larocque, J. (2008): The role of amphibole in the evolution of arc magmas and crust: the case from the Jurassic Bonanza arc section, Vancouver Island, Canada; M.Sc. Thesis, University of Victoria, 115 p.
- Larocque, J. and Canil, D. (2010): The role of amphibole in the evolution of arc magmas and crust: the case from the Jurassic Bonanza arc section, Vancouver Island, Canada; *Contributions to Mineralogy and Petrology*, v. 159, p. 475–492.
- Lee, C.-T.A., Luffi, P., Chin, E.J., Bouchet, R., Dasgupta, R., Morton, D.M., Le Roux, V., Yin, Q.-z. and Jin, D. (2012): Copper systematics in arc magmas and implications for crust-mantle differentiation; *Science*, v. 336, p. 64–68.
- McDonough, W.F. and Sun, S.-s. (1995): The composition of the Earth; *Chemical Geology*, v. 95, p. 223–253.
- Muller, J.E. and Yorath, C.J. (1977): Geology of Vancouver Island; Geological Association of Canada–Mineralogical Association of Canada, Joint Annual Meeting, April 21–24, 1977, Vancouver, British Columbia, Field Trip 7 Guidebook, 53 p.
- Palme, H., and O’Neill, H.S.C. (2014): Cosmochemical estimates of mantle composition; *in* *The Mantle and Core*, R.W. Carlson (ed.), *Treatise on Geochemistry*, Volume 2, Elsevier, p. 1–38, doi:10.1016/B978-0-08-095975-7.00201-1
- Rudnick, R.L. and Gao, S. (2014): Composition of the continental crust; *in* *The Crust*, R.L. Rudnick (ed.), *Treatise on Geochemistry*, Volume 3, Elsevier, p. 1–51, doi:10.1016/B978-0-08-095975-7.00301-6
- Rudnick, R.L. and Fountain, D.M. (1995): Nature and composition of the continental crust: a lower crustal perspective; *Reviews of Geophysics*, v. 33.3, p. 267–309.
- Sillitoe, R.H. (2010): Porphyry copper systems; *Economic Geology*, v. 105, p. 3–41.
- Sinclair, W.D. (2007): Porphyry deposits; *in* *Mineral Deposits of Canada: A Synthesis of Major Deposit-Types, District Metallogeny, the Evolution of Geological Provinces, and Exploration Methods*, W.D. Goodfellow (ed.), Geological Association of Canada, Mineral Deposits Division, Special Publication 5, p. 223–243.
- Smith, D.J. (2014): Clinopyroxene precursors to amphibole sponge in arc crust; *Nature Communications*, v. 5, art. 4329, doi:10.1038/ncomms5329
- Taylor, S.R. (1977): Island arc models and the composition of the continental crust; *in* *Island Arcs, Deep Sea Trenches and Back-Arc Basins*, M. Talwani and W.C. Pitman III (ed.), American Geophysical Union, Maurice Ewing Series, v. 1, p. 325–335.
- Tiepolo, M., Oberti, R., Zanetti, A., Vannucci, R. and Foley, S.F. (2007): Trace-element partitioning between amphibole and silicate melt; *Reviews in Mineralogy and Geochemistry*, v. 67, p. 417–452.